THE JOURNAL OF BIOLOGICAL CHEMISTRY VOL. 287, NO. 42, pp. 35768–35778, October 12, 2012

Mechanistic Studies of Semicarbazone Triapine Targeting Human Ribonucleotide Reductase *in Vitro* and in Mammalian Cells

TYROSYL RADICAL QUENCHING NOT INVOLVING REACTIVE OXYGEN SPECIES[*] [S]

Received for publication, June 30, 2012, and in revised form, August 20, 2012 Published, JBC Papers in Press, August 22, 2012, DOI 10.1074/jbc.M112.396911

Yimon Aye[‡], **Marcus J. C. Long**[§], **and JoAnne Stubbe**[‡¶1]

From the Departments of [‡]*Chemistry and* [¶]*Biology, Massachusetts Institute of Technology, Cambridge, Massachusetts 02139 and the* [§]*Graduate Program in Biochemistry and Biophysics, Brandeis University, Waltham, Massachusetts 02454*

Background: Diferric-tyrosyl radical [(Fe^{III}_2-Y·)(Fe^{III}_2)] cofactor-bearing subunit (β_2) of ribonucleotide reductase is targeted by a Phase-II cancer drug, Triapine (3-AP).
Results: Y· loss precedes iron loss without reactive oxygen species formation.
Conclusion: Fe(II)-(3-AP) inhibits β_2 catalytically resulting in iron-loaded β_2 with a reduced Y·.
Significance: Susceptibility of β_2 to inhibition via Y· reduction by metal complexes implicates a new avenue to develop RNR inhibitors.

Triapine® (3-aminopyridine-2-carboxaldehyde thiosemicarbazone (3-AP)) is a drug in Phase II trials. One of its established cellular targets is the β_2 subunit of ribonucleotide reductase that requires a diferric-tyrosyl-radical [(Fe^{III}_2-Y·)(Fe^{III}_2)] cofactor for *de novo* DNA biosynthesis. Several mechanisms for 3-AP inhibition of β_2 have been proposed; one involves direct iron chelation from β_2, whereas a second involves Y· destruction by reactive oxygen species formed *in situ* in the presence of O_2 and reductant by Fe(II)-(3-AP). Inactivation of β_2 can thus arise from cofactor destruction by loss of iron or Y·. *In vitro* kinetic data on the rates of ^{55}Fe and Y· loss from [($^{55}Fe^{III}_2$-Y·)($^{55}Fe^{III}_2$)]-β_2 under aerobic and anaerobic conditions reveal that Y· loss alone is sufficient for rapid β_2 inactivation. Oxyblot™ and mass spectrometric analyses of trypsin-digested inhibited β_2, and lack of Y· loss from H_2O_2 and $O_2^{\cdot-}$ treatment together preclude reactive oxygen species involvement in Y· loss. Three mammalian cell lines treated with 5 μM 3-AP reveal Y· loss and β_2 inactivation within 30-min of 3-AP-exposure, analyzed by whole-cell EPR and lysate assays, respectively. Selective degradation of apo- over [(Fe^{III}_2-Y·)(Fe^{III}_2)]-β_2 in lysates, similar iron-content in β_2 immunoprecipitated from 3-AP-treated and untreated [^{55}Fe]-prelabeled cells, and prolonged (12 h) stability of the inhibited β_2 are most consistent with Y· loss being the predominant mode of inhibition, with β_2 remaining iron-loaded and stable. A model consistent with *in vitro* and cell-based biochemical studies is presented in which Fe(II)-(3-AP), which can be cycled with reductant, directly reduces Y· of the [(Fe^{III}_2-Y·)(Fe^{III}_2)] cofactor of β_2.

Ribonucleotide reductases (RNRs)[2] supply the monomeric precursors required for DNA replication and repair (1). Two subunits, $(\alpha_2)_m(\beta_2)_n$ (m, n = 1–3) constitute active human (h) RNR (1, 2). α_2 contains the site of nucleotide reduction and binds allosteric effectors that control specificity and reduction rate (1–3). $\beta_2$zoutf; houses a diferric-tyrosyl radical cofactor [(Fe^{III}_2-Y·)(Fe^{III}_2)] (Fig. 1) essential for initiating thiyl radical formation in α_2, which initiates nucleotide reduction (3, 4). RNR plays a central role in nucleic acid metabolism (1, 2, 5, 6) and is the target of three cancer drugs used clinically (7), each targeting a different aspect of the RNR complex mechanism of catalysis and regulation (8–12). This paper focuses on understanding how 3-aminopyridine-2-carboxaldehyde thiosemicarbazone (Triapine® or 3-AP, Fig. 1) specifically inactivates β_2 of hRNR *in vitro* and in cultured mammalian cells.

3-AP has efficacy in a variety of cell lines and animal cancer models (13–15). It is currently in phase II clinical trials (16, 17) resulting in renewed interest in its mechanism of cytotoxicity (18–24). Studies to date suggest that multiple mechanisms of 3-AP are involved in its cytotoxicity (13–15, 18–24). 3-AP is a chelator and readily forms both Fe(II) and Fe(III) complexes (19, 25, 26). The Fe(II)-(3-AP) in the presence of O_2 is able to catalyze generation of ROS (19, 27). The $Fe^{(III)/(II)}$-(3-AP) reduction potential is accessible *in vivo* by endogenous reductants (18, 19, 25, 26).

The diverse properties of 3-AP have resulted in a number of models by which it inhibits RNR. In one model free 3-AP is proposed to chelate the Fe(III) directly from the [(Fe^{III}_2-Y·)(Fe^{III}_2)] within β_2 (14, 28, 29), resulting in RNR inactivation. In a second model 3-AP is proposed to chelate iron from the intracellular iron pool(s) (18, 20) that could interfere with the essential [(Fe^{III}_2-Y·)(Fe^{III}_2)] assembly on β_2 (30). A third model, which is the one currently favored in the literature, is that Fe(III)-(3-AP) is reduced to Fe(II)-(3-AP) by endogenous reductants, which in turn reacts with O_2 and produces ROS that

* This work was supported, in whole or in part, by National Institutes of Health Grant GM29595 (to J. S.). This work was also supported by Damon Runyon Cancer Research Fellowship DRG2015-09 (to Y. A.) and a Howard Hughes Medical Institute international student fellowship (to M. J. C. L.).
[S] This article contains supplemental Materials and Methods, references, Figs. S1–S7, and Table S1.
[1] To whom correspondence should be addressed: Dept. of Chemistry, Dept. of Biology, Massachusetts Institute of Technology, Cambridge, MA 02139. Tel.: 617-253-1814; Fax: 617-258-7247; E-mail: stubbe@mit.edu.

[2] The abbreviations used are: RNR, ribonucleotide reductase; hRNR, human RNR; 3-AP, Triapine®; CHX, cycloheximide; HU, hydroxyurea; ROS, reactive oxygen species; Trx, thioredoxin; Tf, transferrin.

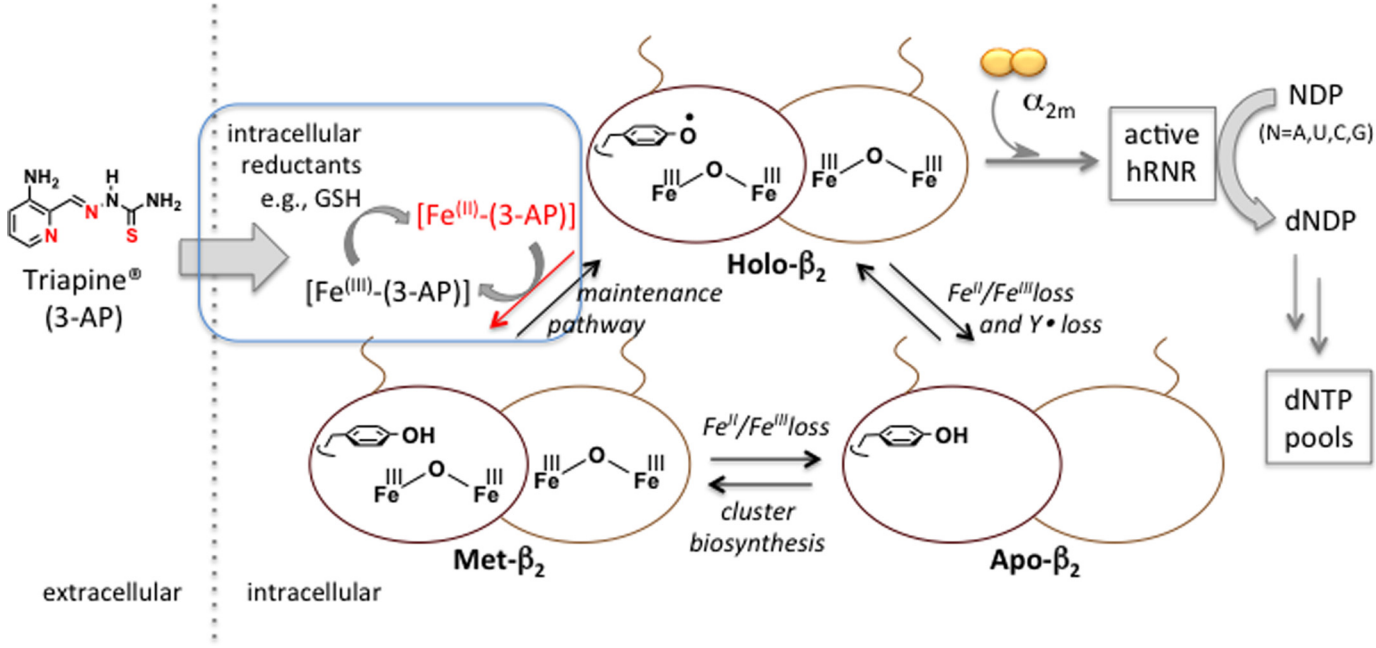

FIGURE 1. **Role of β_2 in hRNR catalysis and impact of β_2-specific inhibition by 3-AP.** Holo-β_2 upon association with $(\alpha_2)_m$ constitutes hRNR that catalyzes nucleoside diphosphate (*NDP*) reduction to dNDPs, one of the key upstream processes that dictates dNTP pool homeostasis. Direct inhibition of β_2 can arise from either loss of Y· (Met-β_2 formation) or $Fe^{III}{}_2$-Y· (apoβ2 formation). Iron-chelating small molecules such as Triapine (3-AP) may also cause indirect inhibition by depletion of intracellular labile iron pool or by Fe(II)-(3-AP)-catalyzed generation of ROS in the presence of O_2. *Blue inset*, this study *in vitro* and in live mammalian cells suggests that β_2-specific inhibition involves reduction of Y· elicited by the active reductant, Fe(II)-(3-AP), catalytically recyclable by intracellular reductants, *e.g.* GSH. This inhibition results in iron-loaded-β_2 with Y· reduced, inferred in our model as Met-β_2 without the need to invoke ROS.

inactivate RNR (21, 27–29). A direct interaction of Y· with O_2^- has also been proposed to lead to β_2 inhibition observed *in vitro* (27–29). Although depletion of the labile iron pools and ROS generation are likely involved in late-stage cytotoxic pathways such as induction of apoptosis (21, 23, 24), we will argue that neither mechanism is likely to be important in RNR-specific inhibition. Previous pharmacological studies by Sartorelli and co-workers (13) and Keppler and co-workers (22) that examined the 3-AP-induced late-stage cytotoxicity in a number of cell lines over 2–4 days noted that blockage of DNA synthesis is induced within the initial hours of 3-AP incubation. Studies by Richardson and co-workers (18) have indicated that cellular iron uptake and efflux are minimally perturbed in 3-AP-treated cultured cells in the first hours of exposure. These interesting findings prompted us to undertake a detailed investigation to understand the mechanism of 3-AP-promoted inhibition of β_2 *in vitro* and in cell culture in the early stages of inhibitor treatment where cell viability remains high, cell cycle is not perturbed, and downstream cytotoxicity is not yet apparent.

Our studies *in vitro* have investigated the effect of 3-AP and its iron complexes on RNR activity, depletion of its essential Y·, and iron loss from the [($Fe^{III}{}_2$-Y·)($Fe^{III}{}_2$)] cluster of β_2 alone and in the active holo-complex [$(\alpha_2)_m(\beta_2$] in a non-cycling or cycling state. The relative rates of Y· loss and iron loss have been measured and vary dependent upon the states of β_2 (β_2 alone, cycling- or non-cycling holo-complex). In all cases, however, Y· loss precedes iron loss, suggesting that β_2-specific inhibition can be explained by the direct reduction of Y·. These data implicate Fe(II)-(3-AP) as the reductant that can rapidly reduce Y·. The observations that Y· loss occurs in the presence and, importantly, in the absence of O_2 and that Y· levels are unaffected by O_2^- or H_2O_2 and the failure to detect oxidative modifications by additional studies using Oxyblot™ technology and mass spectrometry on inhibited β_2 rule out ROS as the basis for Y· reduction.

We have also investigated the effects of 3-AP in K562, COS-1, and hydroxyurea (HU)-resistant TA3 cells on β_2 activity in cell lysates, ^{55}Fe content of β_2 immunoprecipitated from ^{55}Fe-labeled cells, the stability of the inhibited β_2, and the Y· levels in intact cells. Furthermore, Oxyblot™ technology of the whole protein pool failed to reveal differences between 3-AP-treated and untreated cells. Together with *in vitro* data, the rapid and potent RNR inhibition in cells within 30 min of 3-AP treatment is most consistent with the formation of Fe(II)-(3-AP) from free 3-AP with intracellular Fe, which then engages in the direct reduction of the essential Y· of β_2. The inhibition occurs in the period where cell viability remains high, and the activity of α_2 and other abundant iron-dependent enzymes such as aconitase, a sensitive indicator of oxidative stress, are maintained. These findings further underscore the specificity of 3-AP-promoted β_2-specific inhibition and downplay non-specific indirect models discussed above. They provide initial insight into understanding how inhibition of β_2 is involved in the cytotoxic effects of 3-AP.

EXPERIMENTAL PROCEDURES

In Vitro Assays on hRNR—All *in vitro* studies were performed on hRNR subunits recombinantly expressed and purified from *Escherichia coli* (10, 11). Specific activities for CDP reduction were 700–890 nmol $min^{-1}mg^{-1}$ for α and 3000–4100 nmol $min^{-1}mg^{-1}$ for β containing 0.9–1.2 Y·/β_2 and 3.6 iron/β_2. The Y· in the [($Fe^{III}{}_2$-Y·)($Fe^{III}{}_2$)] cluster of β_2 has a $t_{½} \sim 25$ min

at 37 °C in 50 mM Hepes (pH 7.6), 100 mM NaCl. All inhibition data, unless otherwise noted, have thus been adjusted for this intrinsic instability. The presence of 5 mM DTT in the storage buffer is necessary to preserve α_2 activity; thus in all experiments with holo-complex, 85 μM DTT is present. All experiments were carried out at physiological concentrations of subunits (0.5–2.5 μM (monomer) in 3T6 (6, 31–33), COS-1, HeLa, and NIH-3T3 cells (12)), except the EPR experiments where sensitivity limits require 5 μM β_2.

[($^{55}Fe^{III}_2$-Y·)($^{55}Fe^{III}_2$)] Cluster Assembly in β_2—Labeling of the active-site diiron center with ^{55}Fe and subsequent isolation and characterization are detailed in supplemental Materials and Methods. This procedure typically afforded ^{55}Fe-labeled β_2 with 1.0–1.2 Y·/β_2 (quantitated by EPR). The ferrozine assay (34) gave 3.2–3.6 iron/β_2. Non-specifically surface-bound $S = 5/2$ Fe^{III} was quantitated by EPR analysis of the same samples at 77 K involving double integration of the $g = 4.3$ signal relative to Fe^{III}-EDTA standard as detailed previously (35). It was less than 5% (<0.18 iron/β_2) of the total iron. Specific activity of β_2 reconstituted using an identical procedure to that described above with unlabeled $FeCl_3$ was 3000–4100 nmol $min^{-1}mg^{-1}$ of β. Reconstitution and active-site labeling processes were carried out on untagged and His_6-tag β_2 (10) and showed that the tag does not affect activity or the amount of surface-bound iron. All the *in vitro* experiments thus used tagged β_2. All *in vitro* experimental procedures are described in detail in the supplemental Materials and Methods.

Studies in Cultured Cells—COS-1, K562, and HU-resistant TA3 cells were selected as representative mammalian cell lines for the following reasons. COS-1 cells typically yield a relatively large quantity of total protein, and the endogenous β_2 activity per mg of total protein is 1.5–3-fold higher than that typically obtained from HeLa and NIH-3T3. K562 was chosen, as previous studies reveal endogenous levels of Y· can be detected by whole cell EPR (36). TA3 cells further support the data from K562 due to enhanced levels of Y· and also allow study of 3-AP in HU-resistant cells. All in-cell experimental procedures are provided in the supplemental Materials and Methods.

RESULTS

Mechanism of hRNR Inhibition by 3-AP in Vitro—All *in vitro* studies to date on 3-AP-induced inhibition of mouse and hRNR have primarily focused on the analysis Y· loss as a measure of enzyme inactivation (27–29). Because β_2 inhibition can arise from loss of iron, loss of Y·, or both, we have measured independently the effects of 3-AP and its iron complexes on the rates of Y· and active site iron loss.

Time-dependent Inhibition Assays—To establish if RNR activity is depleted in a time-dependent manner and whether this activity loss is associated with β_2 and/or α_2, 0.6 μM β_2 (α_2) was incubated with 0.3, 1, or 5 eq of 3-AP [per $\beta(\alpha)$] for the indicated times and diluted into an assay mixture with a 7-fold excess of α_2 (β_2) and incubated an additional 3 min. The results shown in Fig. 2*A* indicate that with 1 eq or a 5-fold excess of 3-AP per β, >90% of the activity is lost within 10 and 1 min, respectively (Fig. 2*A*). The α_2 subunit activity under the same conditions remains unchanged (Fig. 2*A*), validating that 3-AP is a β_2 subunit-specific inhibitor. Incubation of β_2 with 0.3 eq of 3-AP/β, however, resulted in 50% activity loss at 20 min (Fig. 2*A*), greater than expected if 3-AP itself is the inhibitor. This result suggests that 3-AP has access to iron either from the endogenous loss from β_2 as previously reported in mouse (37) or from nonspecific surface-bound iron associated with the *in vitro* cluster assembly (10, 11). 3-AP-accelerated iron loss has previously been proposed to play a key role in β_2 inhibition (14, 29). If Fe(II)/Fe(III)-(3-AP) is generated, then in the presence of DTT (85 μM) that always accompanies α_2 in the assays, the metal chelate can redox-cycle (19, 25, 26), potentially causing RNR inhibition. These observations are consistent with previous proposals (27–29) that an iron-complex(es) of 3-AP is(are) the true inhibiting species. The kinetics of iron loss from β_2 and whether it is accelerated by 3-AP were, therefore, examined.

Quantitative Assessment of the Rate of Active-site Iron Loss in the Presence and Absence of 3-AP—^{55}Fe-Labeled β_2 was assembled *in vitro* from apoβ2, resulting in specific radioactivity of 652 cpm/nmol of iron with 3.6 iron/β_2 and specific activity in nucleotide reduction and Y· content identical to our previous reports (10, 11). Importantly, EPR analysis showed that the presence of non-specifically surface-bound iron is less than 5% of total iron. Thus ^{55}Fe is predominantly associated with the active site, and our assays monitor the rate of ^{55}Fe loss from this site. A time course for the rate of iron release at 37 °C in the absence and presence of 3-AP was examined under three different sets of conditions: β_2 alone and β_2 with α_2 in a 1:1 molar ratio (1 μM) either in the presence of the allosteric effector ATP (non-cycling holo-complex) or in the presence of the ATP, CDP, thioredoxin (Trx)/thioredoxin reductase/NADPH reducing system (cycling holo-complex). In the absence of 3-AP, the data reveal that the [(Fe^{III}_2-Y·)(Fe^{III}_2)] exhibits very different intrinsic stabilities in the three cases (Fig. 2, *B–D*). When β_2 is alone (Fig. 2*B*) or with α_2 in a non-cycling state (Fig. 2*C*), 20% of the ^{55}Fe is lost over 20 min. Because non-specifically bound ^{55}Fe is <5% that of total iron, the loss detected is associated with loss from metallo-cofactor. The data additionally demonstrate that the intrinsic iron loss is not associated with DTT. DTT is absent in the β_2 alone experiment but present at 85 μM in the non-cycling holo-complex (compare, Fig. 2, *B* and *C*). DTT is required to preserve α_2 stability and is thus carried over from the α_2 storage solution in all *in vitro* studies on the holo-complex. In contrast, 90% of the iron is spontaneously lost in 20 min under cycling conditions (Fig. 2*D*). The observed intrinsic lability in the cycling holo-complex is consistent with previous reports on ^{59}Fe release from the cycling mouse β_2 in the presence of DTT (~60% loss in 30 min) (37). Our data reveal that the intrinsic lability of the cofactor is DTT-independent (Fig. 2, *B* and *C*) and that the cycling state of holo-hRNR provides an additional mechanism for iron loss.

Identical experiments to those described above were then carried out in the presence of 3-AP. In the case of β_2 alone, a 5-eq excess of 3-AP over β (Fig. 2*B*) only elicits 20% iron loss in 20 min, similar to the results in its absence (Fig. 2*B*). This provides compelling evidence that the free ligand does not accelerate active site iron loss on β_2 alone. In contrast, with the addition of α_2, under conditions that result in non-cycling- or cycling-holo-complex, 3-AP greatly enhances the rate of iron release, leading to almost complete loss in 20 min with a $t_{1/2}$ of

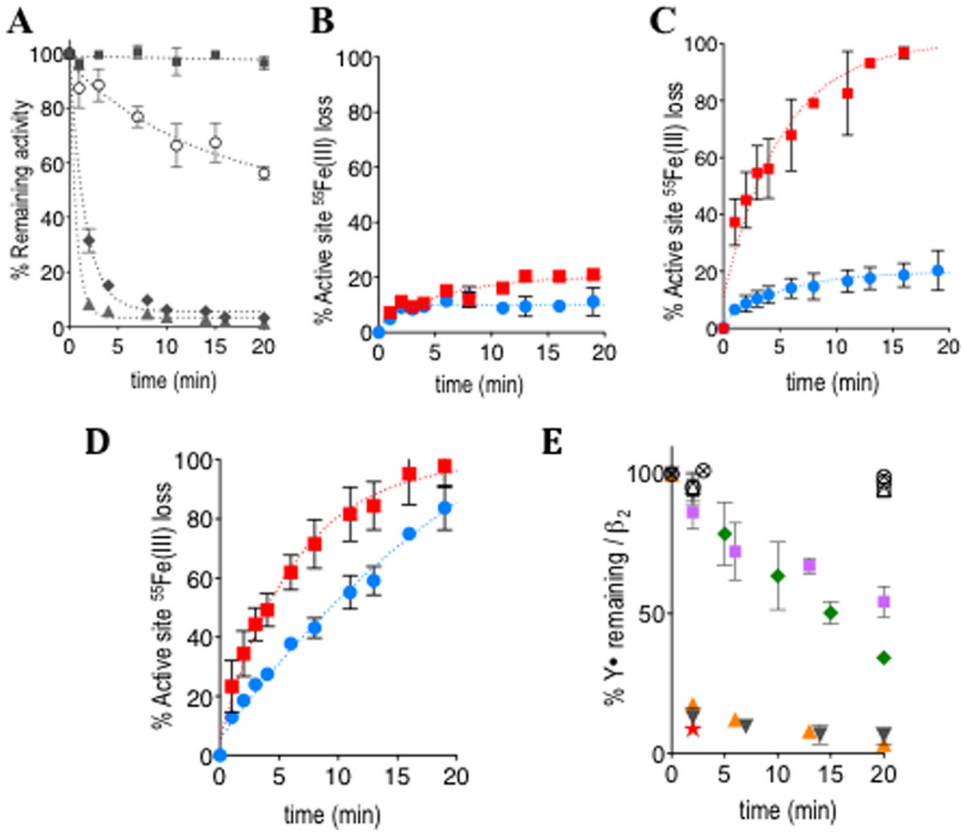

FIGURE 2. Shown are *in vitro* kinetic studies on the α_2 and β_2 activity depletion (*A*), rate of active-site ^{55}Fe loss (*B–D*), or Y· loss (*E*) in β_2. All *error bars* are S.D. over duplicate experiments. *A*, 3-AP-promoted loss of $\alpha_2(\beta_2)$-activity (data have been corrected for intrinsic instability) is shown. Inhibition mixture contained [r-His$_6$-$\alpha(\beta)$]$_2$ = 0.6 μM, [3-AP] = 0, 0.36 (○), 1.2 (♦), or 6.0 (■ for α_2; ▲, for β_2) μM, and 100 μM KCl in 50 μM Hepes (pH 7.6). The assay mixture contained 0.15 μM [r-His$_6$-$\alpha(\beta)$]$_2$, 1.1 μM [r-His$_6$-$\beta(\alpha)$]$_2$, 3 mM ATP, 15 mM $MgCl_2$, and 1.0 mM 5-[^{3}H]CDP, 100 mM KCl, 100 μM Trx, 1 μM Trx reductase, 2 mM NADPH in 50 mM Hepes (pH 7.6). *B–D*, analysis of the rate of ^{55}Fe loss. In all cases, the *red square* and *blue circle*, respectively, designate data with and without 3-AP. *B* is on β_2 alone. The reaction employed 1 μM (r-His$_6$-β)$_2$, 10 μM 3-AP, or 5% of DMSO in double distilled H_2O, 100 mM KCl, and 50 mM Hepes (pH 7.6). *C* is on non-cycling holo-complex. The reaction contained 1 μM (r-His$_6$-α)$_2$, 3 mM ATP, and 15 mM $MgCl_2$ in addition to all the components in *B*. *D* is on the cycling holo-complex. The reaction contained 100 μM Trx, 1 μM Trx reductase, 2 mM NADPH, and 1 mM CDP in addition to all the components in C. *E*, shown is the rate of Y· destruction (corrected for intrinsic Y· decay) analyzed by *in vitro* EPR experiments: by 3-AP alone (green diamond), Fe(III)-(3-AP) (*purple square*), Fe(II)-(3-AP) (*orange triangle*), Fe(III)-(3-AP) in the presence of 5 mM GSH (*black inverted triangle*, *orange star*). The *orange triangle*, *black inverted triangle*, and *orange star* constitute data from strictly anaerobic experiments. (○) and (⊗) indicate the effects on β_2 alone by either 0.5 μM (○) or 50 μM (⊗) H_2O_2 and (△) and (□) by either 50 or 1250 molar excess of $O_2^{\cdot-}$ per β, respectively (generated using xanthine/xanthine oxidase). Representative data shown contained 5 μM (r-His$_6$-β)$_2$ and 50 μM 3-AP or its metal-chelate, except in *orange star*, where 3 μM was used. Also see supplemental Fig. S1*A*.

4.8 min in both cases (Fig. 2, *C* and *D*). The observed increase in loss of iron from the holo-complex in the presence of 3-AP likely implies that formation of the holo-complex may lead to a state(s) that allows the free 3-AP to access iron from the active site, a process not feasible in the case of β_2 alone (Fig. 2*B*). Alternatively, the presence of reductant DTT (carried over with α_2), although having no effect on the intrinsic lability of the cofactor, could redox-cycle the *in situ*-assembled Fe(III)-(3-AP) such that the diferric center in holo-complex is labilized by reduction. Future experiments should provide a mechanistic explanation of these results. Our focus at this time was to determine whether the varied rates and amounts of iron loss observed in the three states of β_2 studied, and whether Y· loss or both are responsible for β_2 inhibition.

Rate of Y· Loss from [(Fe$^{III}_2$-Y·)(Fe$^{III}_2$)]-β_2—EPR studies that monitor Y· were carried out first on β_2 alone under a variety of conditions: with 3-AP alone, with Fe(III)-(3-AP), with Fe(II)-(3-AP) ± O_2, and with Fe(III)-(3-AP) and GSH ± O_2 (Fig. 2*E*). The Y· in hRNR-β_2 is inherently unstable; $t_{1/2}$ of 25 min at 37 °C (11). Control experiments measuring the effect of Fe(II), Fe(III), GSH, and combinations of these on the rate of Y· loss indicated minimal changes relative to inherent instability. The data shown in Fig. 2*E* have been adjusted for the respective intrinsic rates of Y· loss.

In the first experiment 5 eq 3-AP/β was incubated with β_2 alone, and as shown in Fig. 2*E*, 80% of Y· is lost within 20 min. The measured rate of Y· loss induced by the 3-AP alone is similar to that reported for mouse β_2 in the absence of DTT (29). However, comparison of the rate of Y· loss with the rate of ^{55}Fe loss for β_2 alone (Fig. 2*B*) provides the first quantitative evidence that 3-AP effectively targets Y· during a time frame in which its impact on the diferric center remains minimal (Fig. 2, *B versus E*). Our *in vitro* data on β_2 alone thus suggest that Y· quenching is the principle mechanism of enzyme inhibition and leads to iron-loaded β_2.

To further investigate if Y· quenching precedes iron loss in non-cycling holo-complex in the presence of 3-AP, similar EPR analyses were performed and compared with the rates of ^{55}Fe loss (Fig. 2, *C* and *E*). Y· loss was 80% complete in 1 min (supplemental Fig. S1*B*), whereas 40% of total iron was lost in the same timeframe (Fig. 2*C*). Whether the mechanism of iron loss is coupled to Y· loss in this short time frame remains to be estab-

lished. However, if a single mechanism is at play, iron is lost at a rate 5× slower than Y· over the 20-min duration of the assay.

Rapid Y· Reduction Mediated by Fe(II)-(3-AP)—In an effort to understand the form of 3-AP responsible for inhibition of β_2, loss of Y· was also examined in the presence of Fe(III)-(3-AP), Fe(II)-(3-AP) ± O_2, and with Fe(III)-(3-AP) and GSH ± O_2 (Fig. 2*E*). With 5 eq of preassembled Fe(III)-(3-AP) (per β), the rate of Y· loss was similar to the case with 5 eq of free 3-AP/β (Fig. 2*E*). In contrast, when preassembled Fe(II)-(3-AP) was examined, Y· destruction was complete within the first time point. The same rapid Y· loss with a $t_{½}$ of <0.5 min was observed when the experiment was repeated under strictly anaerobic conditions (Fig. 2*E*). These data suggest that Fe(II)-(3-AP) is the active species and that ROS are unlikely to be involved.

To provide additional support for proposed role of Fe(II)-(3-AP), the EPR experiment with preassembled Fe(III)-(3-AP) complex and β_2 alone was replicated in an anaerobic chamber in the presence of 5 mM GSH. GSH was chosen as a reductant due to its physiological role and abundance, and the reported range of redox potentials suggests its ability to reduce Fe(III)-(3-AP) (38). The rapid rate of Y· loss with GSH and in the absence of O_2 (Fig. 2*E*) is consistent with Fe(II)-(3-AP) being the active inhibitor. Importantly, rapid Y· loss is also achieved with substoichiometric amounts of Fe(III)-(3-AP) (0.3 eq/β) when GSH is present (Fig. 2*E*). These results together suggest that reduction of Y· can be elicited by Fe(II)-(3-AP) catalytically without ROS formation. The chemical mechanism and kinetics of Y· reduction will be the focus of future studies.

EPR Analysis of Y· in β_2 Alone in the Presence of H_2O_2 and O_2^-—The effect of H_2O_2 and O_2^- was next evaluated. Earlier studies on *E. coli* β_2 at 25 °C reported H_2O_2-dependent Y· loss (~30% loss by 5.5 mM H_2O_2 in 1 h) (39) as well as irreversible enzyme inactivation by enzymatically generated O_2^- (~80% loss by 3 μM steady-state O_2^- in 0.5 h) (40). Corresponding experiments on eukaryotic β_2 have not been reported. Incubation of 5 μM hRNR β_2 with 50 or 0.5 mM H_2O_2 at 37 °C (Fig. 2*E*) showed no appreciable loss of Y· with respect to controls. Similar experiments in the presence of steady-state concentrations of 0.3 and 3 μM O_2^- generated using xanthine/xanthine oxidase (41–43) revealed that the Y· levels remained unaltered (Fig. 2*E*). Thus H_2O_2 and O_2^- are both incapable of inducing Y· loss at the rate observed in the presence of Fe(II)-(3-AP).

In Vitro Oxyblot™ Analysis of Inhibited β_2 Alone and Cycling- and Non-cycling Holo-complexes—A hallmark of ROS action on proteins via metal-catalyzed oxidation is the formation of protein carbonyls (44). These chemotypes can be probed using Oxyblot™ (Millipore) analysis in which the carbonyls are derivatized to 2,4-dinitrophenyl hydrazones, which are then detected by Western blotting (45). Thus Oxyblots were used to determine if nonspecific oxidative damage could be responsible for β_2 inhibition by 3-AP. β_2 alone and non-cycling- and cycling holo-complexes were incubated with and without 3-AP for 20 min. Proteins in controls and samples with 3-AP were derivatized with 2,4-dinitrophenylhydrazine and subjected to gel electrophoresis followed by Western blot analysis. Protein carbonyls were not detected within β_2 treated with 3-AP under any conditions examined (supplemental Fig. S2*A*). A positive control was carried out with β_2 treated with excess ascorbate and iron. SDS-PAGE/Western analysis revealed that β (47 kDa monomer) in these conditions underwent a gel shift to higher a molecular weight species, presumably associated with cross-linking during oxidative damage. Interestingly, Oxyblot analysis on the cycling holo-complex indicated that Trx reductase was oxidized, further indicating that the Oxyblot could readily detect oxidation; no oxidation, however, was associated with β_2 (supplemental Fig. S2*A*). Omission of 2,4-dinitrophenylhydrazide resulted in complete absence of all the bands. Given the reported sensitivity (fM) of the Oxyblot method, the data imply that Fe(II)-(3-AP)-catalyzed protein oxidation is not involved in β_2 inhibition.

Trypsin Digest LCMS Analysis of Inhibited β_2—To further determine if modification accompanies inhibition of β_2, LCMS analyses were performed on in-gel-digested samples of 5 μM β_2 treated *in vitro* with no 3-AP but 50 μM concentrations of either Fe(II)-(3-AP) or H_2O_2 for 20 min at 37 °C. The resulting peptides were examined for side-chain oxidation (supplemental Table S1*A*) and hydroxylation (supplemental Table S1*B*). Qualitatively, there was no significant difference between these three samples. The modifications detected are likely caused by sample handling during protein isolation, gel electrophoresis, or the in-gel digestion process. The Oxyblot and mass spectrometric data suggest inhibition of β_2 by 3-AP does not result in significant modification of β_2 primary structure.

Mechanism of 3-AP Inhibition in Mammalian Cells—Our attention turned to determine if a similar mechanism occurs in COS-1-, K562-, and HU-resistant TA3 cells exposed to 3-AP.

Loss of β Activity in Cell Lysates from COS-1 and K562 and HU-resistant TA3 Cells Treated with 3-AP—Studies from independent laboratories have reported that cultured cells (HL60 and L1210) exposed to 1–10 μM 3-AP for 0.5–4 h result in complete inhibition of DNA synthesis long before loss of cell viability (2–4 days) (13, 22). Thus our experiments with COS-1 and K562 cells to study the RNR inhibition mechanism were carried out on cells treated with 3-AP (5- 500 μM) over 0.5–3 h where the cells maintained high viability (supplemental Figs. S3 and S4). As shown in supplemental Fig. S5, 30 min of exposure of cells to 3-AP at 5 μM, similar to the *in vivo* concentration for β_2 (~2.5 μM monomer) (6, 31–33), resulted in no detectable β_2 activity in the resulting lysates. Under the same conditions, α_2-activity was unaffected. Similar experiments were also carried out with HU-resistant TA3 cells, previously shown to overexpress β_2 and to have elevated concentrations of Y· by whole-cell EPR analysis (37, 46). Consistent with the higher levels of Y·, our lysate assay data in these cells showed that β_2 activity is ~4-fold higher than that in COS-1 cells (Fig. 3*A* *versus* supplemental Fig. S5*A*). Treatment of TA3 cells with 5 μM 3-AP for 30 min still completely abolished β_2 activity (Fig. 3*A*). Our lysate assay data in all three cell lines thus provided direct evidence that 3-AP promotes rapid loss of RNR activity in live cells and is consistent with previous reports on the early inhibition of DNA synthesis in other cell lines studied (13, 22).

Whole Cell EPR Analysis Links β_2 Inhibition to Y· Loss—Whole cell EPR experiments were undertaken using analogous procedures to the previously published reports (36, 37, 46) to probe whether Y· loss from the [(Fe^{III}_2-Y·)(Fe^{III}_2)] cofactor of β_2 could account for RNR inactivation. Y· was first shown to be detecta-

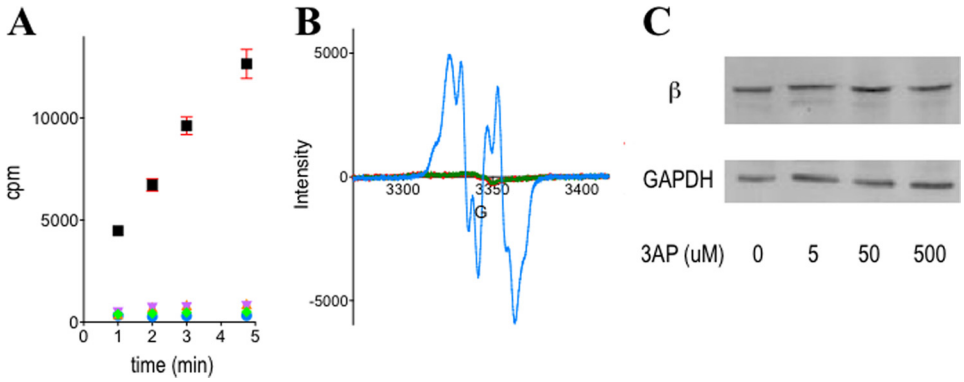

FIGURE 3. **3-AP treatment of HU-resistant TA3 cells results in complete loss of β_2-specific activity (*A*) and Y· (*B*) but no change in β_2 protein levels (*C*).** *A*, β_2 activity in resulting lysates from 30-min-3-AP-treated cells (*black square*, vehicle; *purple inverted triangle*, 500 μM; *orange triangle*, 50 μM; *green diamond*, 5 μM; *blue circle*, background). See supplemental Fig. S5 for the results with COS-1 and K562 cells. *Error bars* are S.D. over two independent experiments. *B*, Y· signal in treated (3 h) (*green lines*, 5 μM; *red lines*, 50 μM) and untreated (*blue dots*) intact TA3 cells analyzed by whole cell EPR. See supplemental Fig. S 6, *C* and *D* for the data at 30 min of treatment in TA3 and K562 cells. *C*, Western blot of β_2 protein levels in treated and untreated TA3 cells at 30 min. See supplemental Fig. S7 for the data from COS-1 and K562 cells. GAPDH was used as the loading control.

ble in untreated K562 and TA3 cells at 30 K (supplemental Fig. S6). In the TA3 cells, the higher level of Y· was reflected in a strong signal that are easily monitored even at 77 K (supplemental Fig. S6*A*), and the signal was identical to that from recombinant [(Fe^{III}_2-Y·)(Fe^{III}_2)]-β_2 reconstituted *in vitro* (supplemental Fig. S6*B*). Treatment of either TA3 or K562 cells with 5 μM 3-AP abolished the Y· in as early as 30 min (Fig. 3*B* and supplemental Fig. S6, *C* and *D*). Note that the lower concentration of Y· in β_2 from K562 cells is accompanied by higher background signals (supplemental Fig. S6*D*) as previously reported (36). Thus whole cell EPR analyses and lysate activity assays together demonstrate that 3-AP targets β_2 in these cells.

Levels of β_2 Are Maintained in 3-AP-treated Cells 12 h Subsequent to Activity Loss—The absence of β_2 activity and loss of Y· could be accompanied by conversion of β_2 to an iron-loaded or apo form (Fig. 1). To address this issue, Western blot analysis was carried out on non-synchronized TA3, K562, and COS-1 cells at 30 min (supplemental Fig. S7). These studies showed that in all three cell lines, β_2 levels were similar to untreated cells (Fig. 3*C* and supplemental Fig. S7). In addition, a time course study showed that β_2 expression was unchanged up to a 12-h period of exposure to 5 μM 3-AP (Fig. 4*B*). Cells also maintained their high viability over this time (supplemental Fig. S3).

Analysis of Stability of Apoβ2 and Holo-β_2 in Mammalian Lysates to Proteasomal Degradation—The *in vivo* data thus far suggest that 3-AP-dependent inhibition is associated with formation of iron-loaded-β_2 but with Y· reduced or apoβ2. However, our *in vitro* analyses suggest that Y· loss alone is sufficient to account for β_2 inhibition (Fig. 2, *B–D*, and supplemental Fig. S1). Two approaches were undertaken to determine the cofactor status in inhibited β_2. The cell cycle-dependent periodicity of mammalian β_2 is regulated by ubiquitin-mediated proteasomal degradation during the passage into mitotic (M) phase (6, 47). This knowledge suggests that β_2 can be primed for degradation by the 26 S proteasome, although the cofactor status of the β_2 being degraded during the M phase remains an outstanding interesting question. We thus started our study using a proteasomal degradation assay (48). COS-1 lysates were chosen to allow comparison with Western blot analysis above. Freshly prepared lysates (1 mg/ml) were supplemented with an ATP-

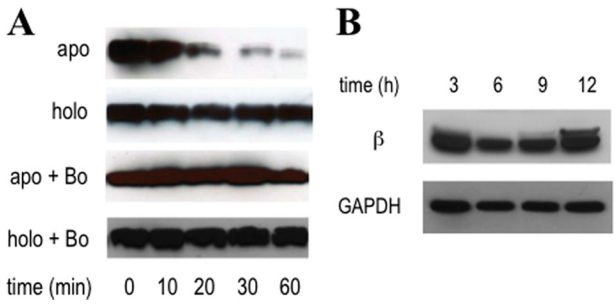

FIGURE 4. **Selective degradation of apoβ2 over holo-β_2 by the proteasome in COS-1 lysates (*A*) and the prolonged stability of inhibited β_2 in 3-AP-treated COS-1 cells (*B*).** *A*, apoβ2 is selectively primed for degradation with $t_{½}$ = 25 min, but holo-β_2 persists. Specific proteasome inhibiting drug, bortezomib (*Bo*), prevents apoβ2 degradation. *B*, β_2 protein levels were maintained over the 12-h treatment of COS-1 cells with 5 μM 3-AP. GAPDH was used as the loading control. High cell viability is maintained throughout this period (supplemental Fig. S3A). Activity depletion occurs within 30 min of exposure to 3-AP (supplemental Fig. S5*A*). Shown here in each diagram are representative Western blots from duplicate sets of experiments.

regenerating system and incubated with either apoβ2 or [(Fe^{III}_2-Y·)(Fe^{III}_2)]-β_2. Aliquots of each reaction were removed at the indicated time points from 0 to 60 min and quenched in Laemmli buffer. Western blot analysis revealed that apoβ2 had a $t_{½}$ of 25 min, whereas the holo-β_2 level remained unaltered at 1 h (Fig. 4*A*). To verify that the proteasome was involved in this degradation, bortezomib, a clinically used proteasome inhibitor (49), was added to separate lysates from the same batch as those shown to degrade apoβ2, and the experiment was repeated (Fig. 4*A*). No degradation was observed, confirming that apoβ2 is targeted by the proteasome.

Stability of Inhibited β_2 Over Prolonged Periods—At this point it is unclear whether β_2 levels (Fig. 4*B*) are unchanged or they appear unchanged due to up-regulation of β_2 expression resulting from 3-AP treatment compensated for by increased β_2 degradation (consistent with apoβ2 formation). Up-regulation in expression of target enzymes upon inhibitor treatment has been reported in mammalian cells (50 and 68) and in many cases and can occur on a 3-h time scale (51). Cycloheximide (CHX), an inhibitor of new protein synthesis (52), was used with 3-AP-treated and untreated cells to gain mechanistic insight. Because β_2 has a $t_{½} \sim 3$ h in mammalian cells (6, 46, 53),

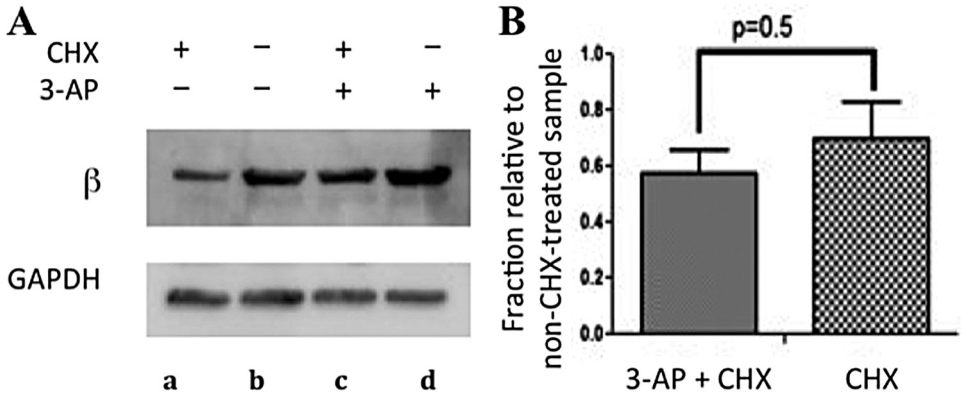

FIGURE 5. **The observed stability of inhibited β_2 is not a coincidental result of reduced stability of β_2 from 3-AP treatment that is offset by the new protein synthesis.** *A*, COS-1 cells were treated with either CHX (0.2 mg/ml) (*lanes a* and *c*) or DMSO (*lanes b* and *d*) for 0.5 h, at which time media were replaced. Half of the plates were re-treated with either 5 μM 3-AP + DMSO (*lane d*) or 5 μM 3-AP + 0.2 mg/ml CHX (*lane c*) for 3-h-labeled, *3-AP+CHX* in *B*. The other half was retreated with either 0.2 mg/ml CHX (*lane a*) or DMSO (*lane b*)-labeled CHX in *B*. *B*, shown is a histogram of data from density analysis of four independent experiments, a representative of which is shown in *A*. *Error bars* are S.D. over quadruplicate sets of experiments.

we opted to compare the effect of 3-AP on the levels of β_2 expression in the presence of CHX. Non-synchronized COS-1 cells in logarithmic phase were treated with CHX (0.2 mg/ml) or DMSO for 0.5 h, at which time the media in half of the CHX-treated samples as well as half of DMSO-treated samples were replaced with media that contained 5 μM 3-AP and CHX (0.2 mg/ml) (Fig. 5*A*, *lane c*) or 5 μM 3-AP only (*lane d*). The data from this set were labeled (*3-AP + CHX*; Fig. 5*B*). The other half of the samples was retreated with CHX (Fig. 5*A*, *lane a*) or DMSO only (*lane b*). The data from this set were labeled *CHX* (Fig. 5*B*). All samples were then incubated for an additional 3 h. This time frame also limits the off-target effects from CHX-induced cytotoxicity (54). Western blot analyses showed that the addition of CHX, as expected, decreased the steady-state level of β_2 by ~60% over 3 h (Fig. 5, *A*, compare *lanes a* and *b*, and *B*, *CHX*), consistent with the reported $t_{½}$ of β_2 in TA3 and 3T6 cells (6, 46, 53). When this experiment was repeated with 5 μM 3-AP (Fig. 5, *A*, compare *lanes c* and *d*, and *B*, *3-AP + CHX*), a similar ~60% decrease in β_2 levels was also observed. Thus β_2 stability was unaffected by 3-AP treatment. Given that apoβ2 appears to be unstable in the lysate degradation assay, iron-loaded β_2 is the most probable species remaining in the 3-AP-treated cells.

^{55}Fe-Pulse Labeling and Immunoprecipitation of β_2 Demonstrates No Change in Iron Loss ± 3-AP-treated Cells—The second approach undertaken to examine the state of inhibited β_2 involves immunoprecipitation from 3-AP-treated and -untreated cells that have been prelabeled with ^{55}Fe. The labile nature of the diferric center revealed by our *in vitro* studies on ^{55}Fe-labeled β_2 (Fig. 2, *B–D*) mandates rapid isolation of β_2. An optimized protocol typically affords ~50 ng of homogeneous β from ~80 × 10^6 K562 cells (Fig. 6*A*). Pulse-labeling was performed according to published protocols (55) using *in vitro* ^{55}Fe-labeled human transferrin (Tf) (2.4 × 10^5 cpm/nmol of iron with 2 iron/Tf), which was added (at 25 μg/ml) to logarithmically growing K562 cells. Subsequent to 18 h of incubation, the ^{55}Fe-labeled Tf-containing media was replaced with fresh media, and the cells were treated with 5 μM 3-AP for 0.5 h or DMSO (control). The cells were then harvested, and the relative levels of ^{55}Fe-labeled β_2 between 3-AP-treated and control

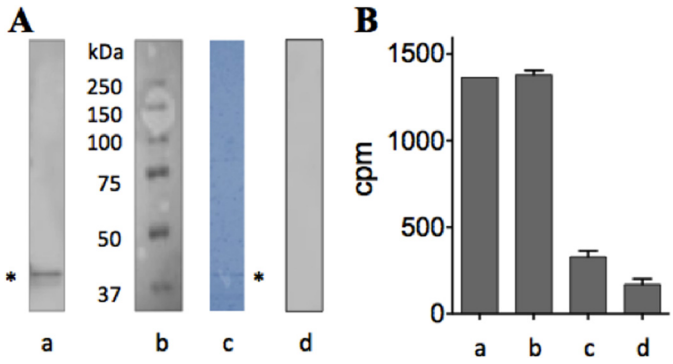

FIGURE 6. **Effect of 3-AP on the diferric cluster of β_2 immunopurified from treated and untreated ^{55}Fe-pulse-labeled K562 cells.** *A*, rapid immunoprecipitation was performed with anti-β_2 antibody (Abcam) conjugated to Protein G-Dyna beads (Invitrogen). *a*, immunoprecipitated human β_2 band (*, monomer, 45 kDa) was confirmed with Western blotting using human β_2-specific antibody (Ab57653). *b*, M_r ladders (Bio-Rad). *c*, PVDF membrane in *a* was stained with Coomassie Brilliant Blue. * indicates immunoprecipitated β monomer. *d*, control as in *a* except buffer replaced Ab57653 but Protein G-Dyna beads were kept. *B*, shown is the amount of radioactivity associated with isolated β_2 subsequent to 30-min treatment of the prelabeled cells with 5 μM inhibitor. Shown are the results from 3-AP-untreated (*a*) and -treated cells (*b*). *c*, treatment was identical to *a*, except anti-β_2 antibody was omitted but the beads were retained. *d*, treatment was *a* except 10 mM HU was added to the lysate. *Error bars* are S.D. over duplicate sets of experiments.

cells were determined using immunoprecipitation. The results are shown in Fig. 6. Importantly, the observed values were appreciably above the non-specifically bound background values obtained in the replica pulldown experiments in which the antibody was omitted, but the resin maintained (Fig. 6, *A*, *lane d*, and *B*, *lane c*). As an additional control, the lysate from the untreated, labeled cells was treated with 10 mM HU during the antibody incubation step, and the immunoprecipitation process was repeated. HU is known to labilize the diiron center from the mouse and hRNR β_2 *in vitro* (56)[3] and in mammalian lysates (57). Consistent with these reports, only background levels of iron are associated with β_2 when HU is added (Fig. 6*B*, *lane d*). These data in addition to the degradation studies suggest that the iron of β_2 is largely retained during the 30 min of exposure of cells to 5 μM 3-AP, although Y· is reduced.

[3] Y. Aye and J. Stubbe, unpublished data.

An Oxyblot of Lysates of 3-AP-treated Cells Shows the Absence of Protein Carbonyls—As shown above *in vitro* (supplemental Fig. S2*A*), further validation of the absence of oxidative carbonylation was probed in whole cell lysates resulting from 3-AP-treated cells and a comparison was made with untreated controls. No change in the extent of carbonylation was observed in any of the cell lines studied (supplemental Fig. S2*B*), suggesting that 3-AP treatment of the mammalian cells over this time period does not induce oxidative damage.

3-AP Is Specific for hRNR over Other Iron/Sulfur-requiring Enzymes: Lack of Inhibition of Aconitase—Given the recent report on the interconnections between iron/sulfur centers, non-heme iron and heme cofactor biogenesis, and iron homeostasis (58, 59), we examined whether 3-AP was selective for β_2 or whether it might affect the activity of other iron-requiring enzymes. Aconitase that contains an essential [4Fe4S] cluster (60) was chosen as a representative enzyme, as its activity is readily assayed in lysates, the cluster is very sensitive to ROS, and one iron is readily lost from the cluster (61). The proposed chelation property of 3-AP could thus affect the availability of labile iron pools from which the iron/sulfur cluster is biosynthesized and repaired (58, 62). Thus, aconitase is a sensitive probe of several mechanisms postulated for 3-AP. However, subsequent to 3 h of treatment of COS-1 cells with 5 μM 3-AP, no changes in aconitase activity relative to the control were observed. These observations are consistent with other data in this study which indicate that 3-AP plays an active role in RNR inhibition. These results further show that the action of 3-AP is β_2-specific.

DISCUSSION

Phase II clinical trials on 3-AP have sparked a resurgence of interest in the mechanisms by which 3-AP and other semicarbazones result in cell cytotoxicity (16, 17). The studies are complex, as 3-AP and similar species are typically excellent iron chelators (19, 20, 25, 26), and the reduction potential of these complexes allows redox cycling under physiological conditions (19, 25, 26), which can result in production of ROS (21, 27–29). 3-AP, in contrast to other iron chelators, does not appear to sequester iron effectively in the cell (18); thus, it is unlikely to be involved in disruption of biosynthesis and repair of many metallo-cofactor-requiring proteins (30, 62, 63). Early studies in cultured cells established that their treatment with 3-AP resulted in rapid DNA inhibition within the initial hours (13, 22) and that this effect was related to loss of activity of RNR known to require a [(Fe^{III}_2-Y·)(Fe^{III}_2)] cofactor (13, 14). This cofactor is common to all class Ia RNRs (holo-β_2, Fig. 1) (3, 4, 30), although the *in vitro* the half-life of the Y· varies from days (*E. coli*) to minutes (*Pseudomonas aeruginosa* and human) (11, 64). In addition, the mouse β_2 under conditions in which deoxynucleoside diphosphates are produced has been reported to spontaneously lose iron (~60% loss in 30 min at 37 °C) (37). Because the [(Fe^{III}_2-Y·)(Fe^{III}_2)] cofactor is essential for RNR activity (3, 4), loss of either Y· or iron cluster results in inhibition.

Studies in cultured cells and xenograft models treated with 3-AP on the other hand have in general focused on assessment of 3-AP-promoted late-stage cytotoxicity (13–15, 18–24, 28, 29). These data suggest that multiple pathways are operative. Postulated mechanisms include deficiency in DNA lesion repair (15), depletion of intracellular iron storage pools (18, 20), ROS-mediated oxidative damage (21, 24, 27–29), and initiation of apoptotic signals (21, 23, 24). Our data now provide a window into the initial period of 3-AP treatment of cells before loss of regulation at multiple levels impact cell viability. A unified model results from comparison of *in vitro* and cell culture studies despite many remaining questions that need to be resolved.

In vitro—The currently favored model for the mechanism of RNR inhibition by 3-AP *in vitro* is that Fe(III)-(3-AP) can be reduced to Fe(II)-(3-AP) by DTT in assay buffers (27–29) or β_2 itself (29) and generate ROS that reduce the Y·. Yen and co-workers (27) studying hRNR β_2 alone by EPR analysis showed complete loss of Y· subsequent to a 30-min incubation with a catalytic amount of Fe(II)-(3-AP) (preassembled in the presence of excess DTT). Under the same conditions, Fe(III)-(3-AP) without DTT resulted in ~60% Y· loss, whereas 3-AP alone resulted in ~40% Y· loss (see Fig. 4 in Yen and co-workers (27)). These results are similar to our EPR data shown in Fig. 2*E*. Yen and co-workers (27) further showed using a 5,5-dimethyl-1-pyrroline-*N*-oxide as a radical trap that incubation of Fe(II)-(3-AP) with O_2 generates ROS and that superoxide dismutase and catalase partially prevented Y· loss. From all their data they concluded that O_2 is important in Y· destruction. Their complex experimental protocol, however, involved preincubation of Fe(II)-(3-AP) for 30 min with catalase alone or in combination with superoxide dismutase before addition to β_2 followed by a further 30-min incubation. The experimental design (27) and the observation that DTT, Fe(II), and O_2 can rapidly regenerate Y· (65) suggest that an alternative interpretation of their results is possible; that is, that Y· is regenerated.

Gräslund and co-workers (29) has also reported time-dependent Y· loss on mouse β_2 alone. Their EPR data in the presence of DTT (see Fig. 6 in Gräslund and co-workers (29)) support Fe(II)-(3-AP) as the active species in Y· reduction, consistent with Yen and co-workers (27, 28) and our own data. However, as in Yen and co-workers (27, 28), Gräslund and co-workers (29) favor the importance of ROS in Y· reduction. This proposal was based on the observation that they observed 100% loss in Y· in 5 min at 37 °C with substoichiometric amounts of Fe(III)-(3-AP) relative to β_2 but only 20% loss under anaerobic conditions (see Fig. 6*a* in Gräslund and co-workers (29)). The source of reducing equivalents essential for reduction of Fe(III)-(3-AP) to Fe(II)-(3-AP) was suggested to be mouse β_2 itself. We note that with Fe(III)-(3-AP) and O_2, neither our laboratory (Fig. 2*E*) nor Yen and co-workers (27) see 100% Y· loss, although the possibility remains that hRNR-β_2 is distinct from the mouse enzyme. The basis for the differences in the results remains unresolved. Finally, although both the Yen (27, 28) and Gräslund laboratories (29) have suggested that 3-AP can bind to β_2, in the former case based on binding experiments with 3-[^{3}H]AP and the latter case based on molecular docking and computational analysis, in neither case is the proposal compelling.

We propose an alternative model, consistent with our biochemical studies, that accommodates most of the previously reported results. Our kinetic data on Y· and ^{55}Fe loss from β_2 suggest that rapid inhibition of hRNR-β_2 results from reduction of Y· by Fe(II)-(3-AP) by outer sphere electron transfer (Fig. 2, *B*–*E*). This mechanism also can account for catalytic

cycling of this reductant but does not involve O_2 (Fig. 2*E*). Our studies further suggest that met-β_2 is likely generated (Fig. 2*B*) and that this state persists for 20 min, the duration of the assay. Given recent studies on the *P. aeruginosa* β (64), however, we cannot rule out the possibility that $Fe^{II}{}_2$ is formed and remains tightly bound. Our additional experiments reveal that presence of α_2 appears to allow 3-AP to remove the iron from the holo-complex, although the rate of iron loss is slower than Y· loss (Fig. 2, *C* and *D*, supplemental Fig. S1*B*). Finally, efforts to detect evidence for damage to the inhibited β_2 using oxyblot methods (supplemental Fig. S2*A*) and mass spectroscopy analysis of peptides of in-gel-trypsinized β_2 (supplemental Table S1) failed to reveal protein damage that could account for its inhibition. Thus our data *in vitro* show that the inhibition of β_2 occurs without the need to invoke ROS formation. We also observe a distinction between the effects of 3-AP on Y· reduction and chelation of active-site iron (Fig. 2, *B--E*). A detailed mechanism of Fe(II)-(3-AP) reduction of the Y· remains to be established *in vitro*.

In Vivo—Our studies in cell culture further support our *in vitro* mechanism for 3-AP-mediated β_2 inhibition that occurs in the initial hours of drug treatment (0.5–4 h) (13, 22). Evidence is provided from whole cell EPR methods to monitor Y· (Fig. 3*B*, supplemental Fig. S6, *C* and *D*), ^{55}Fe-labeled Tf labeling, and immunoprecipitation of the inhibited β_2 to assess iron content (Fig. 6) and oxyblot experiments of the 3-AP treated cells (supplemental Fig. S2*B*). Our results demonstrate that Y· loss occurs in multiple cell lines after only a 30-min exposure to 3-AP (Fig. 3*B*, supplemental Fig. S6, *C* and *D*). Assays of accompanying cell lysates revealed no detectable RNR activity (Fig. 3*A*, supplemental Fig. S5) or iron loss in the same time frame (Fig. 6*B*). Finally, no enhanced oxidation due to 3-AP treatment of the live cells was detected (supplemental Fig. S6*B*).

In the cell the actual state(s) of β_2 (holo-complex *versus* β_2 alone) has not been reported. Our studies indicate that the final state of β_2 is iron-loaded with its Y· reduced (Figs. 4*A* and 6). The inhibited state of β_2 is surprisingly stable even under conditions where new protein synthesis is inhibited (Fig. 5). Our findings suggest that apoβ_2 is not the end product in 3-AP-treated cells. Finally, α_2 is also present in cells, conditions where 3-AP can remove iron from β_2 in a holo-complex based on our *in vitro* findings (Fig. 2, *C* and *D*). Thus, although a portion of β_2 may undergo iron loss, it may be reloaded, giving rise to the observed protein stability in 3-AP-treated cells (Figs. 4*B* and 5). Preservation of the diiron center in β_2 is consistent with previous studies with SK-N-MC cells treated with 50 μM 3-AP for 3 h which revealed that iron uptake from ^{59}Fe-labeled Tf (~20%) and iron release from ^{59}Fe pulse-labeled cells (25%) were both minimal relative to the other iron chelators studied (18). Consistent with these results, whole cell EPR analyses of 3-AP-treated K562 cells (5 or 500 μM) after 0.5, 3, and 12 h showed no change in the size of the intracellular $g = 4.3$ signals between the treated and untreated cells (data not shown). These observations contrast to the phenotype typically observed when chelation and depletion of intracellular iron pools are in operation (36).

Our studies thus raise interesting questions about the mechanisms by which the diiron cluster of β_2 persists and whether the [($Fe^{III}{}_2$-Y·)($Fe^{III}{}_2$)]-β_2 can be regenerated by a maintenance pathway *in vivo*, with the Y· continually being re-reduced by cycling Fe(II)-(3-AP). The identification of a small molecule that can negatively intercept the regeneration of active cofactor in living mammalian cells (Fig. 1) may ultimately shed light on the [($Fe^{III}{}_2$-Y·)($Fe^{III}{}_2$)] cluster biosynthetic and maintenance pathways (30).

Our model is that Fe(II)-(3-AP) is the active species involved in β_2 inhibition (Fig. 1). This proposal is in accord with the reported detection of EPR signals ($g = 2$) in peripheral blood mononuclear cells collected from patients treated with 3-AP (66) within 2 h of treatment, proposed to be iron- and copper-bound 3-AP. Given the intracellular prevalence of iron relative to Cu (63) and the stability constants for 3-AP (19, 24, 25, 29), Fe(II)-(3-AP) is the most likely active species. Our *in vitro* studies with ^{55}Fe-labeled β_2 suggest the protein itself is capable of providing at least catalytic amounts of iron in all states of β_2 (Fig. 2, *B–D*); *in vivo*, however, multiple sources of iron are present. In the continued presence of free ligand in cultured cells, RNR inhibition can persist by the redox cycling capacity of Fe(II)/(III) complex (19, 25, 26), facilitated by intracellular reductants such as GSH (38). Finally, although our model (Fig. 1) primarily focuses on targeting β_2 alone, our data *in vitro* and in non-synchronized cells suggest that the holo-complex is also susceptible to 3-AP-promoted inhibition by direct Y· reduction (Fig. 2, *C* and *D* and supplemental Fig. S1*B*).

Our findings demonstrate that Y· within hRNR β_2 in any state (alone or non-cycling or cycling holo-complex) is highly susceptible to reduction while being stable to a range of reactive small-molecule oxidants. This observation is significant because a pool of β_2 unbound to $(\alpha_2)_m$ almost certainly exists in cells, and our *in vitro* data show that this form of β_2 is relatively inert to iron chelation, at least by 3-AP. Thus to design more effective semicarbazone anticancer agents, the efficiency of the reduction of hRNR Y· by the semicarbazone Fe(III)/(II) complexes should be considered alongside other pharmacokinetic properties. Furthermore, because Y· is highly susceptible to reduction, alternative reductants/radical quenchers should be investigated as potential β_2 inhibitors (19). Finally, our studies provide a simple series of experiments that can be used to distinguish between ROS effects and Y· reduction both *in vitro* and in cells, allowing a more thorough evaluation/optimization of other semicarbazones as potential therapeutics.

Acknowledgments—We thank Professor Lars Thelander of Umeå University, Sweden, for the generous provision of hydroxyurea-resistant TA3 cell lines and Dr. Ioannis Papayannopoulos, Principal Scientist and Director of Proteomics Facility, Koch Institute for Integrative Cancer Research at the Massachusetts Institute of Technology, for discussion and help with the analysis of mass spectrometry data.

REFERENCES

1. Nordlund, P., and Reichard, P. (2006) Ribonucleotide reductases. *Annu. Rev. Biochem.* **75,** 681–706
2. Hofer, A., Crona, M., Logan, D. T., Sjöberg, B. M. (2012) DNA building blocks. Keeping control of manufacture. *Crit. Rev. Biochem. Mol. Biol.* **47,** 50–63
3. Stubbe, J., and van Der Donk, W. A. (1998) Protein radicals in enzyme catalysis. *Chem. Rev.* **98,** 705–762
4. Stubbe, J., Nocera, D. G., Yee, C. S., and Chang, M. C. (2003) Radical initiation in the class I ribonucleotide reductase. Long-range proton-cou-

pled electron transfer. *Chem. Rev.* **103,** 2167–2201
5. Zhou, B. B., and Elledge, S. J. (2000) The DNA damage response. Putting checkpoints in perspective. *Nature* **408,** 433–439
6. Thelander, L. (2007) Ribonucleotide reductase and mitochondrial DNA synthesis. *Nat. Genet.* **39,** 703–704
7. Shao, J., Zhou, B., Chu, B., and Yen, Y. (2006) Ribonucleotide reductase inhibitors and future drug design. *Curr. Cancer Drug Targets* **6,** 409–431
8. Krakoff, I. H. (1975) in *Antineoplastic and Immunosuppressive Agents, Part II* (Sartorelli, A. C., and Johns, D. G., eds.) pp. 789–792, Springer-Verlag New York Inc., New York
9. Gandhi, V., and Plunkett, W. (2006) in *Cancer Drug Discovery and Development: Deoxynucleoside Analogs in Cancer Therapy* (Peters, G. J., ed.) pp. 153–171, Humana Press, Totowa, NJ
10. Wang, J., Lohman, G. J., and Stubbe, J. (2007) Enhanced subunit interactions with gemcitabine 5′-diphosphate inhibit ribonucleotide reductases. *Proc. Natl. Acad. Sci. U.S.A.* **104,** 14324–14329
11. Aye, Y., and Stubbe, J. (2011) Clofarabine 5′-di and -triphosphates inhibit human ribonucleotide reductase by altering the quaternary structure of its large subunit. *Proc. Natl. Acad. Sci. U.S.A.* **108,** 9815–9820
12. Aye, Y., Brignole, E. J., Long, M. J., Chittuluru, J., Drennan, C. L., Asturias, F. J., and Stubbe, J. (2012) Clofarabine targets the large subunit (α) of human ribonucleotide reductase in live cells by assembly into persistent hexamers. *Chem. Biol.* **19,** 799–805
13. Cory, J. G., Cory, A. H., Rappa, G., Lorico, A., Liu, M. C., Lin, T. S., and Sartorelli, A. C. (1994) Inhibitors of ribonucleotide reductase. Comparative effects of amino- and hydroxyl-substituted pyridine-2-carboxaldehyde thiosemicarbazones. *Biochem. Pharm.* **48,** 335–344
14. Finch, R. A., Liu, M. C., Cory, A. H., Cory, J. G., Sartorelli, A. C. (1999) Triapine (3-aminopyridine-2-carboxaldehyde thiosemicarbazone (3-AP)). An inhibitor of ribonucleotide reductase with antineoplastic activity. *Adv. Enzyme Regul.* **39,** 3–12
15. Finch, R. A., Liu, M., Grill, S. P., Rose, W. C., Loomis, R., Vasquez, K. M., Cheng, Y., and Sartorelli, A. C. (2000) Triapine (3-aminopyridine-2-carboxaldehyde-thiosemicarbazone). A potent inhibitor of ribonucleotide reductase activity with broad spectrum antitumor activity. *Biochem. Pharm.* **59,** 983–991
16. Nutting, C. M., van Herpen, C. M., Miah, A. B., Bhide, S. A., Machiels, J. P., Buter, J., Kelly, C., de Raucourt, D., and Harrington, K. J. (2009) Phase II study of 3-AP triapine in patients with recurrent or metastatic head and neck squamous cell carcinoma. *Ann. Oncol.* **20,** 1275–1279
17. Traynor, A. M., Lee, J. W., Bayer, G. K., Tate, J. M., Thomas, S. P., Mazurczak, M., Graham, D. L., Kolesar, J. M., and Schiller, J. H. (2010) A phase II trial of Triapine (NSC# 663249) and gemcitabine as second line treatment of advanced non-small cell lung cancer. Eastern cooperative oncology group study 1503. *Invest. New Drugs* **28,** 91–97
18. Chaston, T. B., Lovejoy, D. B., Watts, R. N., and Richardson, D. R. (2003) Examination of the antiproliferative activity of iron chelators. Multiple cellular targets and the different mechanism of action of triapine compared with desferrioxamine and the potent pyridoxal isonicotinoyl hydrazine analogue 311′. *Clin. Cancer Res.* **9,** 402–414
19. Richardson, D. R., Kalinowski, D. S., Richardson, V., Sharpe, P. C., Lovejoy, D. B., Islam, M., and Bernhardt, P. V. (2009) 2-Acetylpyridine thiosemicarbazones are potent iron chelators and antiproliferative agents. Redox activity, iron complexation, and characterization of their antitumor activity. *J. Med. Chem.* **52,** 1459–1470
20. Yu, Y., Wong, J., Lovejoy, D. B., Kalinowski, D. S., and Richardson, D. R. (2006) Chelators at the cancer coalface. Desferrioxamine to triapine and beyond. *Clin. Cancer Res.* **12,** 6876–6883
21. Merlot, A. M., Kalinowski, D. S., and Richardson, D. R. (2012) Novel chelators for cancer treatment. Where are they now? *Antioxid. Redox. Signal.* [Epub ahead of print]
22. Kowol, C. R., Trondl, R., Heffeter, P., Arion, V. B., Jakupec, M. A., Roller, A., Galanski, M., Berger, W., and Keppler, B. K. (2009) Impact of metal coordination on cytotoxicity of 3-aminopyridine-2-carboxaldehyde thiosemicarbazone (triapine) and novel insights into terminal dimethylation. *J. Med. Chem.* **52,** 5032–5043
23. Alvero, A. B., Chen, W., Sartorelli, A. C., Schwartz, P., Rutherford, T., and Mor, G. (2006) Triapine (3-aminopyridine-2-carboxaldehyde thiosemicarbazone) induces apoptosis in ovarian cancer cells. *J. Soc. Gynecol. Investig.* **13,** 145–152
24. Yu, Y., Gutierrez, E., Kovacevic, Z., Saletta, F., Obeidy, P., Suryo Rahmanto, Y., and Richardson, D. R. (2012) Iron chelators for the treatment of cancer. *Curr. Med. Chem.* **19,** 2689–2702
25. Enyedy, E. A., Nagy, N. V., Zsigó, Kowol, C. R., Arion, V. B., Keppler, B. K., and Kiss, T. (2010) Comparative solution equilibrium study of the interactions of copper (II), iron (II) and zinc (II) with triapine (3-aminopyridine-2-carboxaldehyde thiosemicarbazone) and related ligands. *Eur. J. Inorg. Chem.* **2010,** 1717–1728
26. Enyedy, É. A., Primik, M. F., Kowol, C. R., Arion, V. B., Kiss, T., and Keppler, B. K. (2011) Interaction of triapine and related thiosemicarbazones with iron(III)/(II) and gallium(III). A comparative solution equilibrium study. *Dalton Trans.* **40,** 5895–5905
27. Shao, J., Zhou, B., Di Bilio, A. J., Zhu, L., Wang, T., Qi, C., Shih, J., and Yen, Y. (2006) A ferrous-triapine complex mediates formation of reactive oxygen species that inactivate human ribonucleotide reductase. *Mol. Cancer Ther.* **5,** 586–592
28. Zhu, L., Zhou, B., Chen, X., Jiang, H., Shao, J., and Yen, Y. (2009) Inhibitory mechanisms of heterocyclic carboxaldehyde thiosemicarbazones for two forms of human ribonucleotide reductase. *Biochem. Pharm.* **78,** 1178–1185
29. Popovi-Bijeli, A., Kowol, C. R., Lind, M. E., Luo, J., Himo, F., Enyedy, E. A., Arion, V. B., and Gräslund, A. (2011) Rinoculeotide reductase inhibition by metal complexes of triapine (3-aminopyridine-2-carboxaldehyde-thiosemicarbazone). A combined experimental and theoretical study. *J. Inorg. Biochem.* **105,** 1422–1431
30. Cotruvo, J. A., and Stubbe, J. (2011) Class I ribonucleotide reductase. Metallocofactor assembly and repair *in vitro* and *in vivo*. *Annu. Rev. Biochem.* **80,** 733–767
31. Akerblom, L., Ehrenberg, A., Gräslund, A., Lankinen, H., Reichard, P., and Thelander, L. (1981) Overproduction of the free radical of ribonucleotide reductase in hydroxyurea-resistant mouse fibroblast 3T6 cells. *Proc. Natl. Acad. Sci. U.S.A.* **78,** 2159–2163
32. Engström, Y., Eriksson, S., Jildevik, I., Skog, S., Thelander, L., and Tribukait, B. (1985) Cell cycle-dependent expression of mammalian ribonucleotide reductase. *J. Biol. Chem.* **260,** 9114–9116
33. Håkansson, P., Hofer, A., and Thelander, L. (2006) Regulation of mammalian ribonucleotide reduction and dNTP pools after DNA damage and in resting cells. *J. Biol. Chem.* **281,** 7834–7841
34. Fish W. W. (1988) Rapid colorimetric micromethod for the quantitation of complexed iron in biological samples. *Methods Enzymol.* **158,** 357–364
35. Bou-Abdallah, F., and Chasteen, N. D. (2008) Spin concentration measurements of high-spin ($g' = 4.3$) rhombic iron(III) ions in biological samples. Theory and application. *J. Biol. Inorg. Chem.* **13,** 15–24
36. Cooper, C. E., Lynagh, G. R., Hoyes, K. P., Hider, R. C., Cammack, R., and Porter, J. B. (1996) The relationship of intracellular iron chelation to the inhibition and regulation of human ribonuleotide reductase. *J. Biol. Chem.* **271,** 20291–20299
37. Nyholm, S., Mann, G. J., Johansson, A. G., Bergeron, R. J., Gräslund, A., and Thelander, L. (1993) Role of ribonucleotide reductase in inhibition of mammalian cell growth by potent iron chelators. *J. Biol. Chem.* **268,** 26200–26205
38. Barycki, J. J. (2008) in *Redox Biochemistry* (Banerjee, R., and Becker, D., eds) pp. 11–21, John Wiley & Sons, Inc., Hoboken, NJ
39. Sahlin, M., Sjöberg, B. M., Backes, G., Loehr, T., and Sanders-Loehr, J. (1990) Activation of the iron-containing B2 protein of ribonucleotide reductase by hydrogen peroxide. *Biochem. Biophys. Res. Commun.* **167,** 813–818
40. Gaudu, P., Nivière, V., Pétillot, Y., Kauppi, B., and Fontecave, M. (1996) The irreversible inactivation of ribocucleotide reductase from *Escherichia coli* by superoxide radicals. *FEBS Lett.* **387,** 137–140
41. McCord, J. M., and Fridovich, I. (1969) Superoxide dismutase. An enzymatic function for erythrocuprein (hemocuprein). *J. Biol. Chem.* **244,** 6049–6055
42. Del Maestro, R. F., Björk, J., and Arfors, K. E. (1981) Increase in microvascular permeability induced by enzymatically generated free radicals. *Microvasc. Res.* **22,** 239–254
43. Imlay, J. A., and Fridovich, I. (1991) Assay of metabolic superoxide production in *Escherichia coli*. *J. Biol. Chem.* **266,** 6957–6965

44. Stadtman, E. R. (1993) Oxidation of free amino acids and amino acid residues in proteins by radiolysis and by metal-catalyzed reactions. *Ann. Rev. Biochem.* **62,** 797–821
45. Hernebring, M., Brolén, G., Aguilaniu, H., Semb, H., and Nyström, T. (2006) Elimination of damaged proteins during differentiation of embryonic stem cells. *Proc. Natl. Acad. Sci. U.S.A.* **103,** 7700–7705
46. Eriksson, S., Gräslund, A., Skog, S., Thelander, L., and Tribukait, B. (1984) Cell cycle-dependent regulation of mammalian ribonucleotide reductase. The S-phase correlated increase in subunit M2 is regulated by *de novo* protein synthesis. *J. Biol. Chem.* **259,** 11695–11700
47. Chabes, A. L., Pfleger, C. M., Kirschner, M. W., and Thelander, L. (2003) Mouse ribonucleotide reductase R2 protein. A new target for anaphase-promoting complex-Cdh1-mediated proteolysis. *Proc. Natl. Acad. Sci. U.S.A.* **100,** 3925–3929
48. Hershko, A., and Ciechanover, A. (1998) The ubiquitin system. *Ann. Rev. Biochem.* **67,** 425–479
49. Adams, J., Kauffman, M. (2004) Development of the proteasome inhibitor Velcade® (Bortezomib). *Cancer Invest.* **22,** 304–311
50. Stargell, L. A., Heruth, D. P., Gaertig, J., and Gorovsky, M. A. (1992) Drugs affecting microtubule dynamics increase α-tubulin mRNA accumulation via transcription in *Tetrahymena thermophila*. *Mol. Cell. Biol.* **12,** 1443–1450
51. Hsieh, Y. C., Skacel, N. E., Bansal, N., Scotto, K. W., Banerjee, D., Bertino, J. R., and Abali, E. E. (2009) Species-specific differences in translational regulation of dihydrofolate reductase. *Mol. Pharmacol.* **76,** 723–733
52. Obrig, T. G., Culp, W. J., McKeehan, W. L., and Hardesty, B. (1971) The mechanism by which cycoheximide and related glutarimide antibiotics inhibit peptide synthesis on reticulocyte ribosomes. *J. Biol. Chem.* **246,** 174–181
53. Chabes, A., and Thelander, L. (2000) Controlled protein degradation regulates ribonucleotide reductase activity in proliferating mammalian cells during the normal cell cycle and in response to DNA damage and replication blocks. *J. Biol. Chem.* **275,** 17747–17753
54. Christner, C., Wyrwa, R., Marsch, S., Küllertz, G., Thiericke, R., Grabley, S., Schumann, D., and Fischer, G. (1999) Synthesis and cytotoxic evaluation of cycloheximide derivatives as potential inhibitors of FKBP12 with neuroregenerative properties. *J. Med. Chem.* **42,** 3615–3622
55. Fuller, S. D., and Simons, K. (1986) Transferrin receptor polarity and recycling accuracy in "tight" and "leaky" strains of Madin-Darby canine kidney cells. *J. Cell Biol.* **103,** 1767–1779
56. Nyholm, S., Thelander, L., and Gräslund, A. (1993) Reduction and loss of the iron center in the reaction of the small subunit of mouse ribonucleotide reductase with hydroxyurea. *Biochemistry* **32,** 11569–11574
57. McClarty, G. A., Chan, A. K., Choy, B. K., and Wright, J. A. (1990) Increased ferritin gene expression is associated with increased ribonucleotide reductase gene expression and the establishment of hydroxyurea resistance in mammalian cells. *J. Biol. Chem.* **265,** 7539–7547
58. Mühlenhoff, U., Molik, S., Godoy, J. R., Uzarska, M. A., Richter, N., Seubert, A., Zhang, Y., Stubbe, J., Pierrel, F., Herrero, E., Lillig, C. H., and Lill R. (2010) Cytosolic monothiol glutaredoxins function in intracellular iron sensing and trafficking via their bound iron-sulfur cluster. *Cell Metab.* **12,** 373–385
59. Zhang, Y., Liu, L., Wu, X., An, X., Stubbe, J., and Huang, M. (2011) Investigation of *in vivo* diferric tyrosyl radical formation in *Saccharomyces cerevisiae* Rnr2 protein. Requirement of Rnr4 and contribution of Grx3/4 and Dre2 proteins. *J. Biol. Chem.* **286,** 41499–41509
60. Rose, I. A., and O'Connell, E. L. (1967) Mechanism of aconitase action. *J. Biol. Chem.* **242,** 1870–1879
61. Gardner, P. R., Nguyen, D. D., White, C. W. (1994) Aconitase is a sensitive and critical target of oxygen poisoning in cultured cells and in rat lungs. *Proc. Natl. Acad. Sci. U.S.A.* **91,** 12248–12252
62. Lill, R. (2009) Function and biogenesis of iron-sulfur proteins. *Nature* **460,** 831–838
63. Hentze, M. W., Muckenthaler, M. U., and Andrews, N. C. (2004) Balancing acts. Molecular control of mammalian iron metabolism. *Cell* **117,** 285–297
64. Torrents, E., Westman, M., Sahlin, M., and Sjöberg, B. M. (2006) Ribonucleotide reductase modularity. Atypical duplication of the ATP-cone domain in *Pseudomonas aeruginosa*. *J. Biol. Chem.* **281,** 25287–25296
65. Thelander, L., and Gräslund, A. (1983) Mechanism of inhibition of mammalian ribonucleotide reductase by the iron chelate of 1-formylisoquinoline thiosemicarbazone. *J. Biol. Chem.* **258,** 4063–4066
66. Kolesar, J. M., Schelman, W. R., Geiger, P. G., Holen, K. D., Traynor, A. M., Alberti, D. B., Thomas, J. P., Chitambar, C. R., Wilding, G., and Antholine, W. E. (2008) Electron paramagnetic resonance study of peripheral blood mononuclear cells from patients with refractory solid tumors treated with Triapine®. *J. Inorg. Biochem.* **102,** 693–698
67. Deleted in proof
68. Berg, R. W., Ferguso, P. J., DeMoor, J. M., Vincen, M. D., and Koropatnick, J. (2002) The means to an end of tumor cell resistance to chemotherapeutic drugs targeting thymidylate synthase. Shoot the messenger. *Curr. Drug Targets* **3,** 297–309